SRF cavities surface investigation and defect removal technologies

Matsievskiy Sergey
National Research Nuclear University "MEPhI", Moscow

September 3, 2013

Abstract

For abstract part of this report I would like to place an abstract story by Daniel Charms
Its name is "Four illustrations on how a new idea dumbfounds a man that was not ready for it"
I
The Writer: I am a writer!
The Reader: And I think you are crap!
(The Writer stands there for a few minutes shocked by this new idea, falls dead. He is carried away.)
II
The Painter: I am a painter!
The Worker: And I think you are crap!
(The Painter went pale as a canvas, and shaking like a little leaf, suddenly dies. He is carried away.)
III
The Composer: I am a composer!
Ivan Rublev: And I think you are crap!
(The composer, breathing heavily, dies. He is carried away.)
IV
The Chemist: I am a chemist!
The Physicist: And I think you are crap!
(The Chemist didn't say another word and falls heavily on the floor.)

Contents

1. Introduction 3
   - 1.1. Particle accelerator superconductive cavities 3
   - 1.2. Electrical gradient limiting factors and quench 4
2. Quench positioning 5
   - 2.1. T-mapping system 5
   - 2.2. Second sound phenomena 6
   - 2.3. Second sound system 7
3. Defect properties investigation 12
   - 3.1. OBAHT system 12
   - 3.2. Replicas of defects 13
4. Defects removal 15
   - 4.1. Centrifuge polishing 15
   - 4.2. Diagnostics after polishing 17
5. Summary 19
6. References 19

1. Introduction

Discoveries in particle physics in the last decades were only possible with experiments at particle accelerators providing high-energy particle beams and collisions. The importance of particle accelerators is undeniable.

Nowadays superconductivity in particle accelerators is rapidly growing field of study because of overall greater efficiency of such accelerators. Therefore the research for increasing of superconductive cavity performance is very important and perspective for future particle accelerators.

DESY FLA/ILC group is conducting research of superconductive cavity defects, limiting cavity performance and their elimination for future ILC project.

1.1. Particle accelerator superconductive cavities

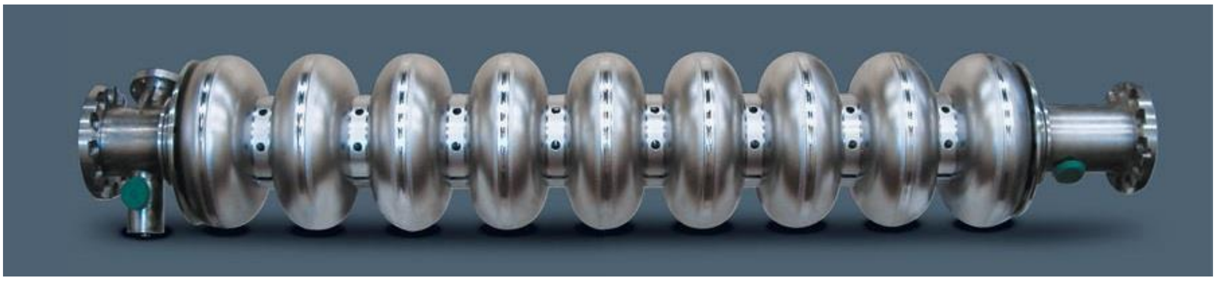

Figure 1 TESLA-shape Superconductive radiofrequency (SRF) cavity

Superconductive cavities, in comparison to regular cavities, operated on room temperature have low ohmic losses, which implies high quality factors and accelerating gradients for these cavities. For most of modern superconductive lepton accelerators, TESLA type cavities are used. These cavities operate on TM_{010} mode (Figure 2). Niobium(Nb) is used as superconductor. Its critical temperature T_c=9.3 K.

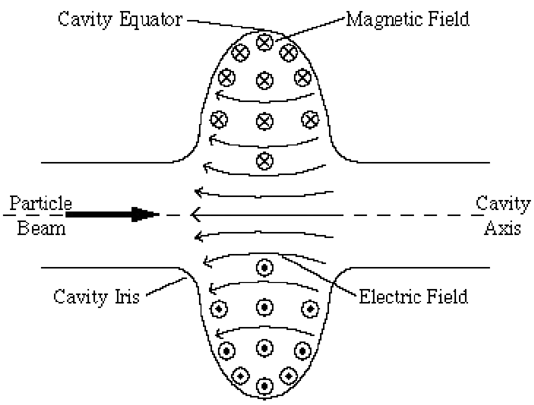

Figure 2 Field distribution in TESLA cavities (parts of cavity specified)

For increasing of system efficiency and simplification of power insert, superconductive cavities for linear particle accelerators consist of nine cells, combined in to one cryogenic tank (see Figure 3).

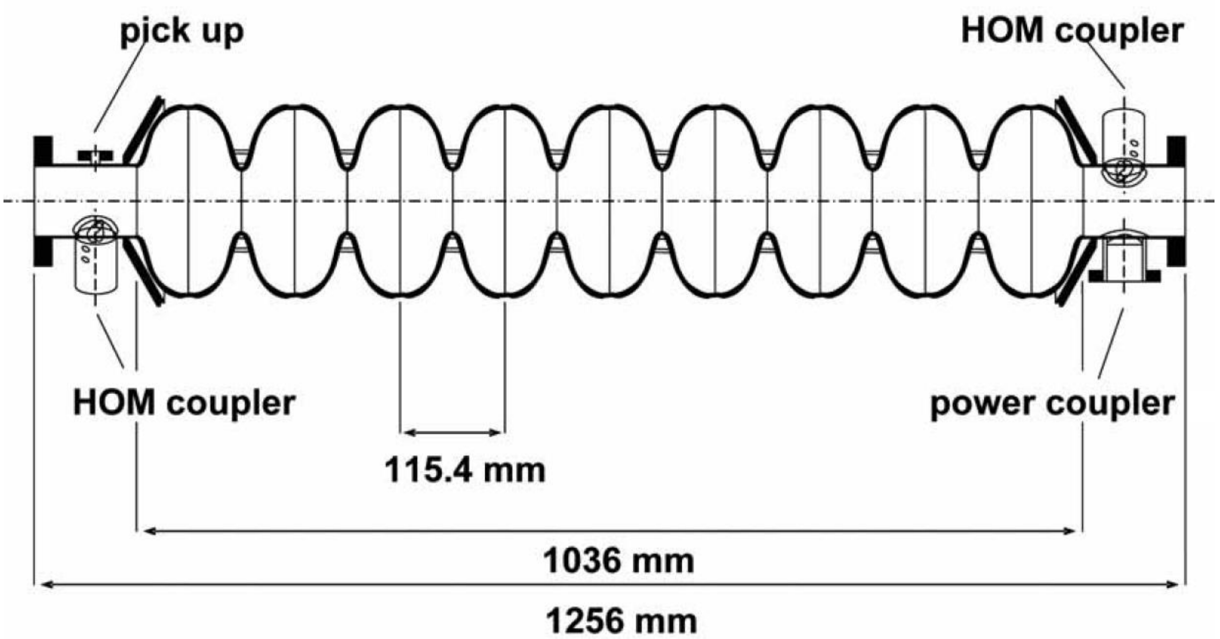

Figure 3 9-cell 1.3 GHz SRF cavity drawing (without cryogenic tank)

In the Table 1 specifications for superconductive cavies for EXFEL and ILC projects are shown.

Table 1 Cavity specifications for EXFEL and ILC projects [1, 2]

	EXFEL	ILC
Operating frequency	1.3 GHz	1.3 GHz
Nominal accelerating field	>23.6 MV/m	>31.5 MV/m
Unloaded quality factor Q_0	$>1 \cdot 10^{10}$	$>1 \cdot 10^{10}$
Number of 1.3 GHz 9-cell cavities	800	16000
Operating temperature	2K	2K

1.2. Electrical gradient limiting factors and quench

Cavity performance is usually described by Q_0 over E_{acc} plot (Example on Figure 4).

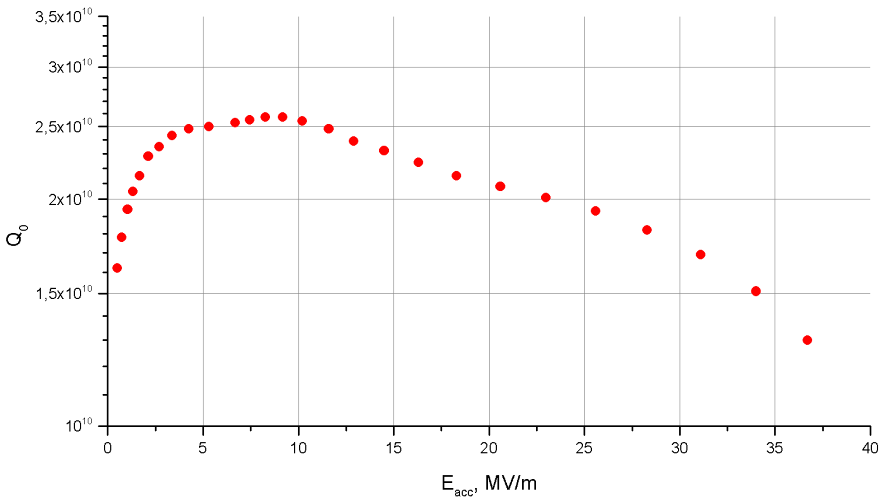

Figure 4 Q_0 over E_{acc} plot at 1.8K

Quench – phenomenon of superconductivity loss by SRF cavities due to local heating. If a small part of niobium loses its superconductivity, power, stored in cavity, additionally heats it and everything near it. Quench is a common phenomenon in a superconducting cavity and often limits the accelerating gradient of the cavity. There are number of accelerating gradient limiting factors: multipacting, , field emission [3]. Today multipacking and Q-disease are usually avoided, and the main reason is surface contamination and defects.

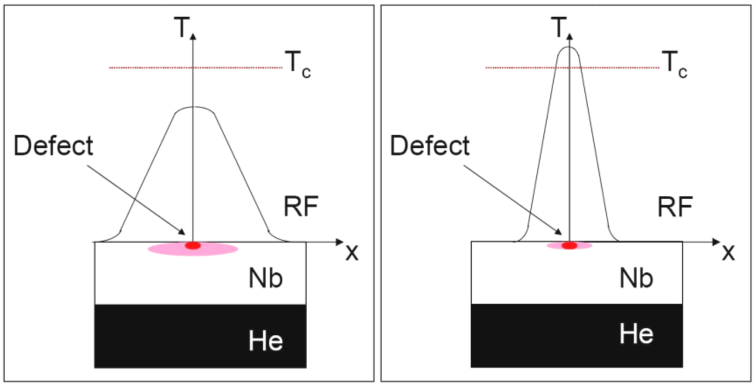

Figure 5 Quenching process

2. Quench positioning

There are two quench positioning system, used in FLA/ILC laboratory: T-mapping and Second sound systems. They are described further.

2.1. T-mapping system

T-mapping system uses temperature detectors for making a temperature map of cavity surface to find heating spots. For temperature detectors NTC thermistors are used.

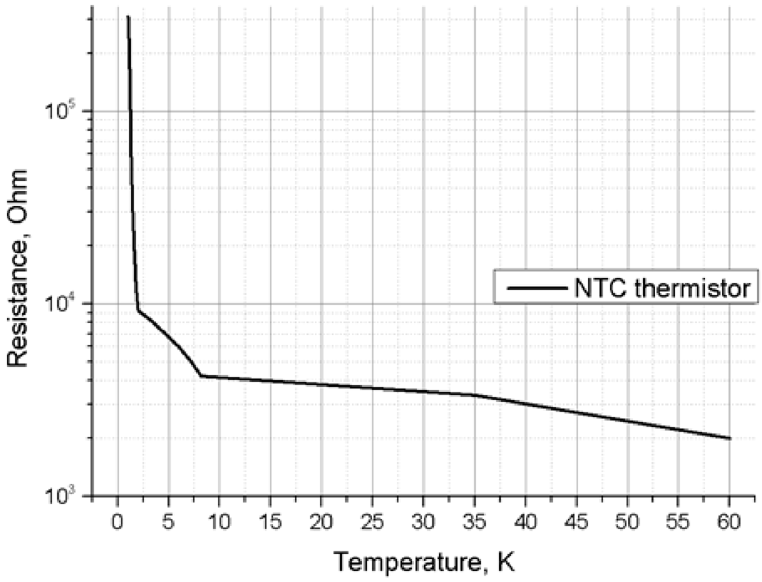

Figure 6 NTC thermistor resistance curve

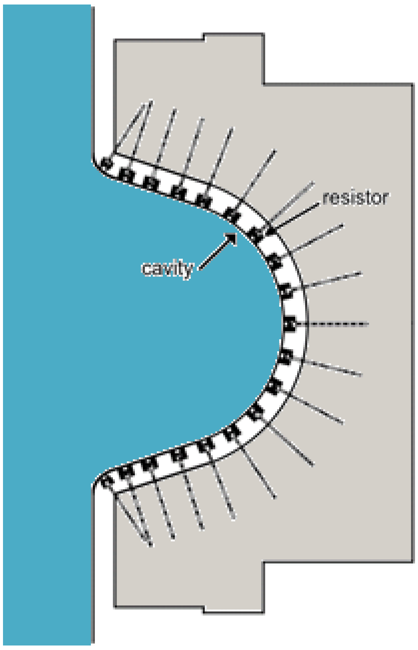

Figure 7 Thermistor positioning on the cell

Detectors are installed on rotating beams, pressed to cavity by springs. System rotates around the cavity and at the event of quench makes snapshot of detectors resistance. After conversion temperature map is assembled. Spot with the highest temperature is a quench spot.

Figure 8 Assembled T-mapping system

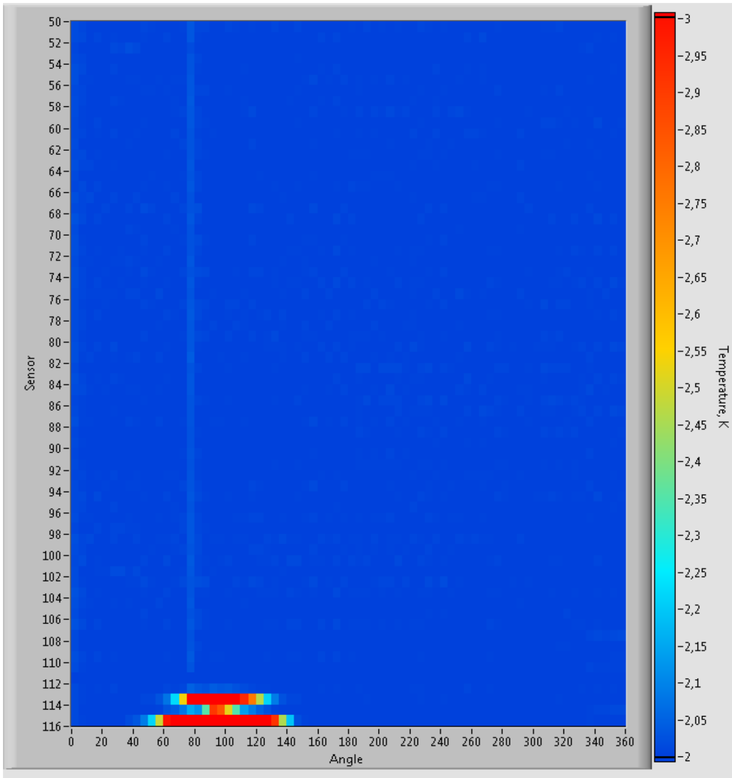

Figure 9 Example of temperature map for cavity

2.2. Second sound phenomena

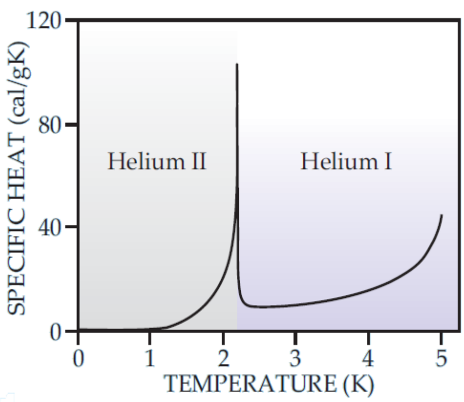

Figure 10 Phases of helium [6]

At the temperatures below 2.17 K liquid helium starts to transit to phase, called helium II. This phase, according to the two-fluid model, consists of two phases of helium: normal (n) and superfluid (s) [4, 5].

Anomalously high thermal conductivity of He II is due to the fact that the heat can be transferred in it by the motion of the normal component in the absence of full mass flow, compensated by counter flow of superfluid component, which is carrying no heat.

Second sound – weakly damped oscillations of temperature and entropy in superfluid helium (HeII). The existence of second sound is due to the appearance of additional degrees of freedom in HeII as a result of the phase transition to the superfluid state of helium; in conventional media as temperature fluctuations are damped at distances of the order of the wavelength. Propagation velocity of second sound v_2 is determined from equations of hydrodynamics of a superfluid (two-component model). If anomalously low helium thermal expansion factor is neglected, the wave of second sound is an oscillation only temperature T and entropy S. Density r and pressure p remain constant. Spread of second sound is not accompanied by the transfer of matter $(j = \rho_s v_s + \rho_n v_n)$, moreover the superfluid and normal components with densities ρ_s and ρ_n oscillate with speeds v_s and v_n in opposite phases.

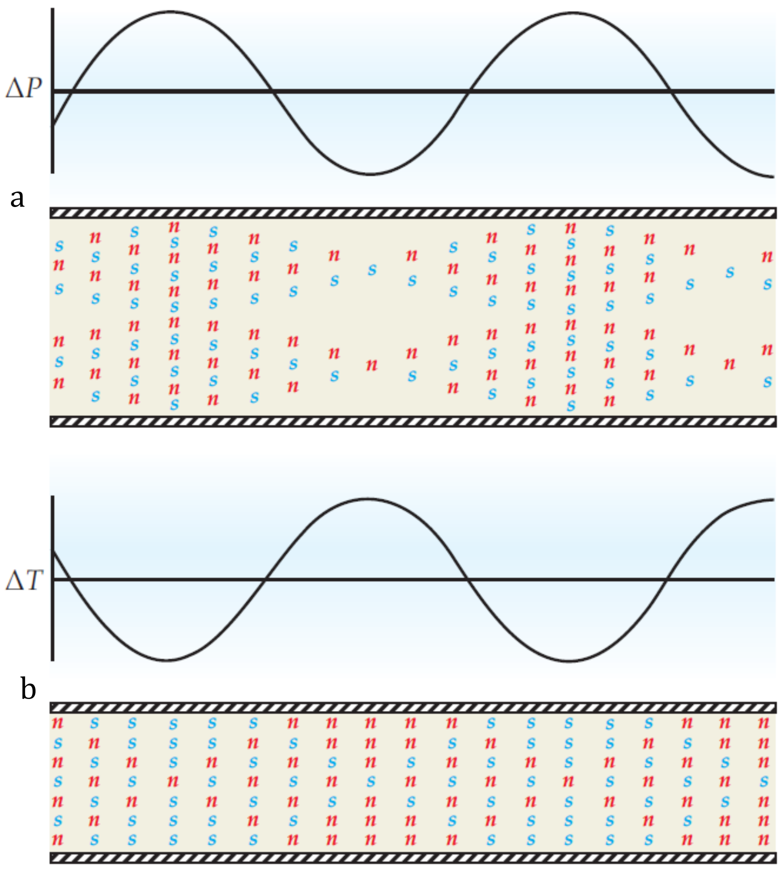

Figure 11 First (a) and second (b) sound waves and helium phases [6]

$v_1^2 \approx \left(\frac{\partial P}{\partial \rho}\right)_s$ – first sound velocity

$v_2^2 \approx \frac{TS^2\rho_s}{C\rho_n}\nabla^2 T$ – second sound velocity

Propagating velocity of second sound wave in helium at temperature $T = 1.8\,K$ is approximately 20 m/s.

2.3. Second sound system


Figure 12 OST detector

The detection of the second sound wave can be done by using thermometers for measuring the small temperature change. Another method is to detect the propagating wave of the phase transition directly with capacitor microphone-like oscillating superleak transducers (OST) (see Fig. 12). These devices consist of a body made of aluminium, a centered brass electrode electrically isolated from the body and a thin porous diaphragm sputtered with a thin gold layer at the outside. A voltage is applied between the brass electrode and the body/diaphragm, and the voltage changes due to the capacitance change, due to helium I and helium II counterflow. This signal is amplified and measured (See figure 13).

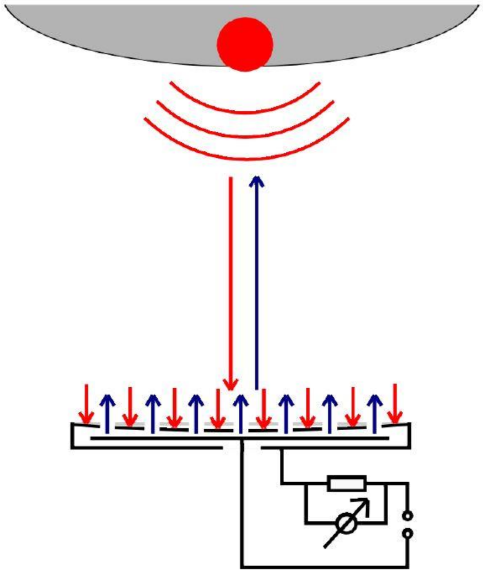

Figure 13 Principal of quench detecting using second sound wave

Figure 14 Assembled second sound system (OSTs in one row are circled red)

In the vertical cold tests at DESY, a set of sixteen OSTs was used since 2011. Number of OSTs was increased to eighteen for better quench localization in the middle section of cavity. Now there are two OSTs per cell equator. Detectors are evenly placed in four rows of cold RF test insert.

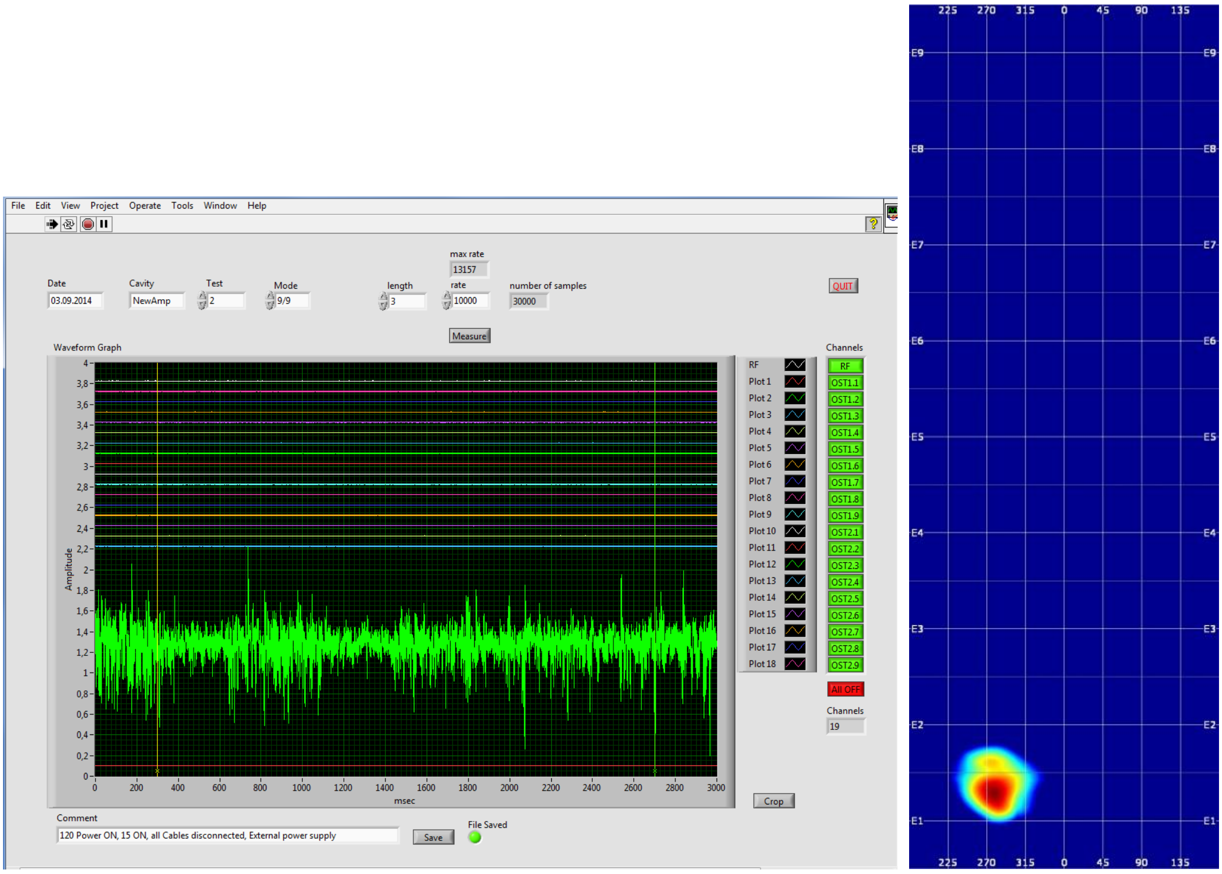

Figure 15 New DAQ software on the left, quench location output on the right

Before modification the data collection was done by a pair of multiplexed USB-ADCs with a constant sampling rate of 10 kHz per channel and differential input. Acquiring the second sound signals and the reflected power was done with a MATLAB R program. New version of program is written with the LabVIEW software, which natively supports ADC (Figure 15). Sample rate changeover feature was added as well as channel choosing (with maximum conversion speed of 256 thousand samples per second). That allows receiving data from each OST individually with maximum conversion speed of ADC. Input mode of ADC was changed from differential to single-ended. It eliminated the need for having two ADCs and increased maximum sampling rate.

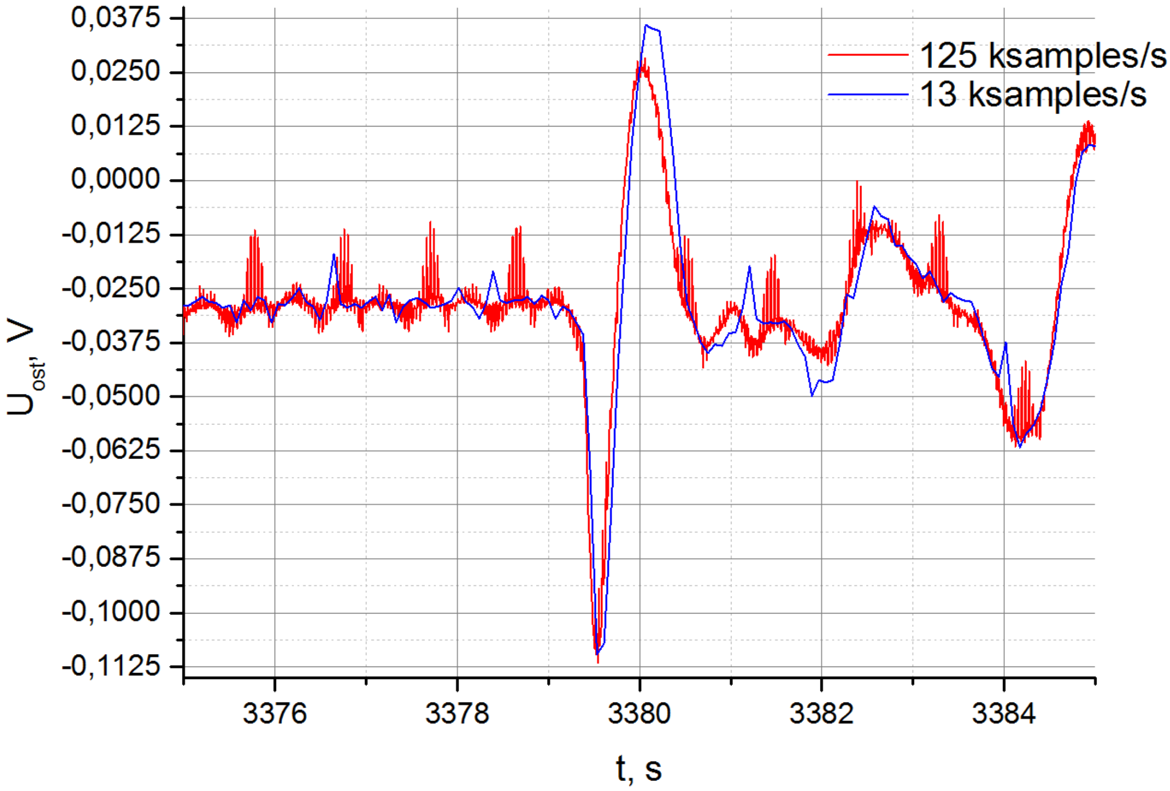

Figure 16 Signal from OST detectors converted different sample rates (13 and 125 kSamples/s)

Time of quench was determined by reflected power of cavity. If the quench limit of the cavity is reached, the reflected power rises abruptly. The time difference between reflected power rise and the oscillation onset on the OSTs is a propagation time of the second sound wave. Knowing the positions of OST detectors quench position can be calculated. Example of calculated quench location is shown on figure 15.

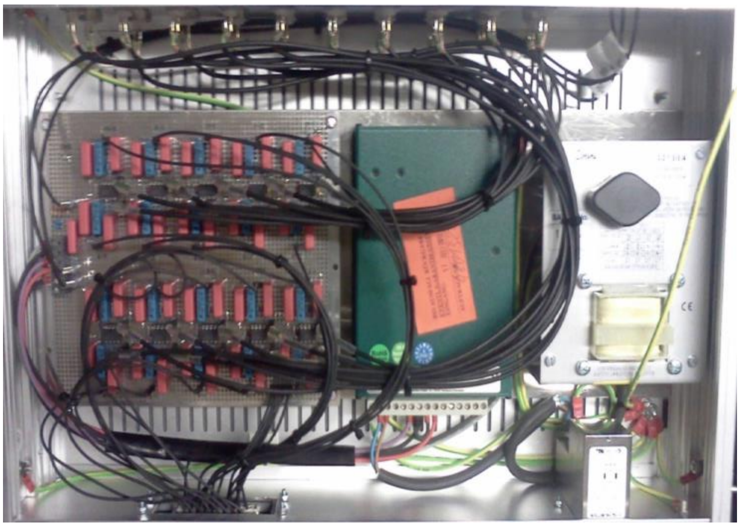

Figure 17 Photo of amplifier box
(Wires are not shielded and located close to unshielded power supply)

Big problem with second sound system was signal front determination due to the high noise level. Was determined that noise came mostly from unshielded power source inside of the amplifier. To eliminate noise power supply and amplifying circuits were separated by a metal wall.

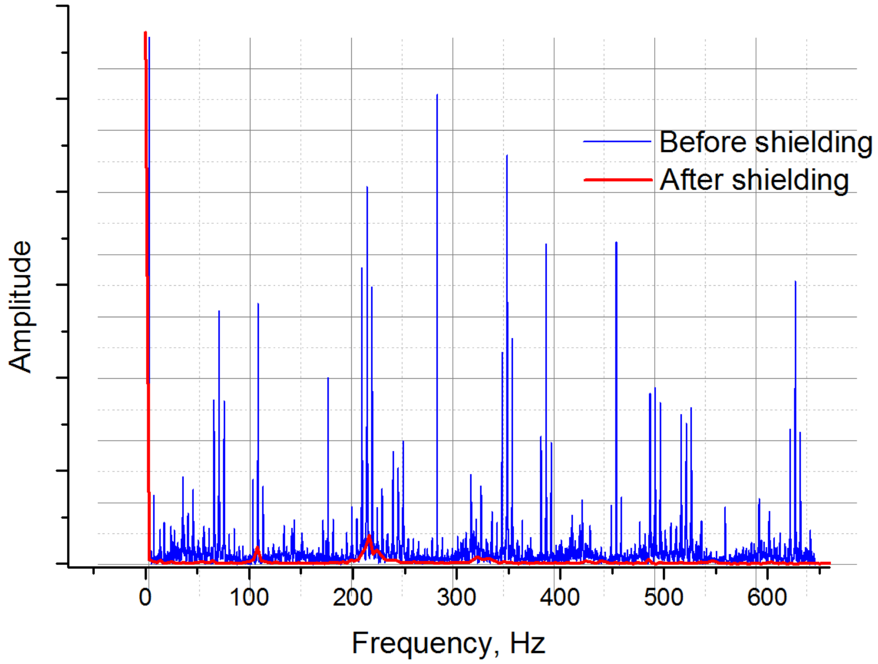

Figure 18 Noise frequency response for initial and shielded amplifier

After shielding, amplifier was tested and some noise remained. Frequency of noise changed with sample rate change.

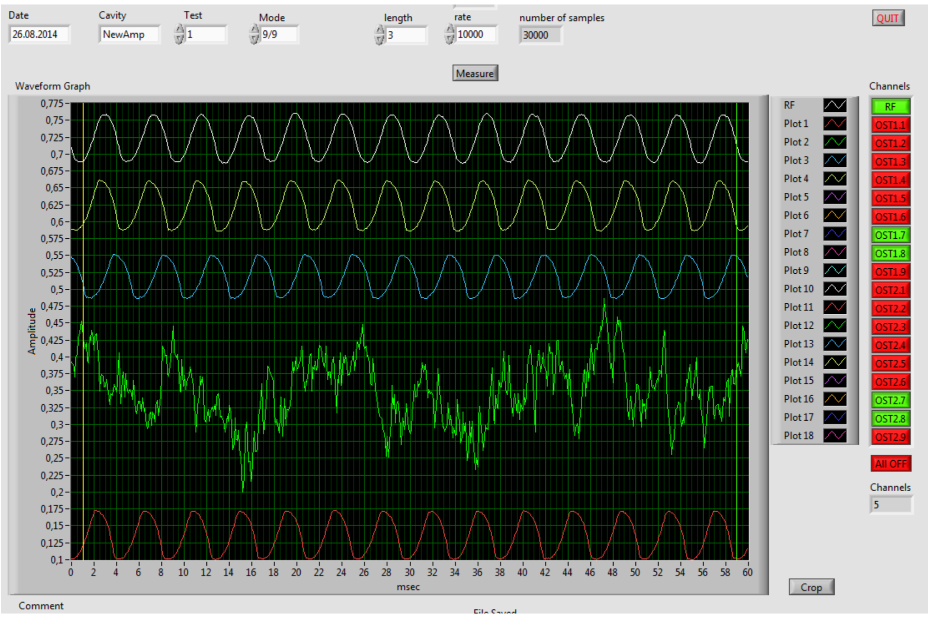

Figure 19 Environment noise, captured with OST (green) and internal noise of amplifier

After examination with osciloscpoe was discovered that this is 50 kHz noise, coused by unstable power supply of amplifier. Gating of this high frequency noise with different sampling rate appeared as noise frequency change. After stabalizing of amplifier power supply this noise was eliminated.

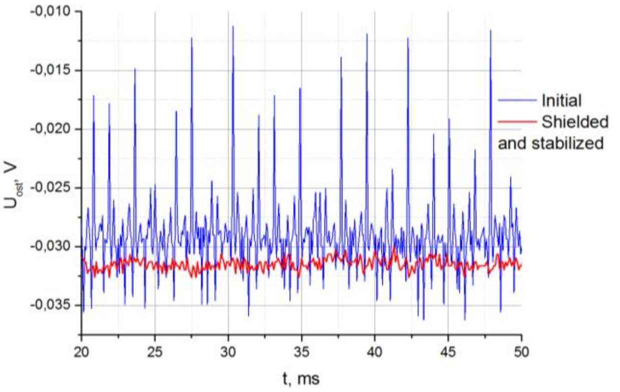

Figure 20 Noise level before and after amplifier modification

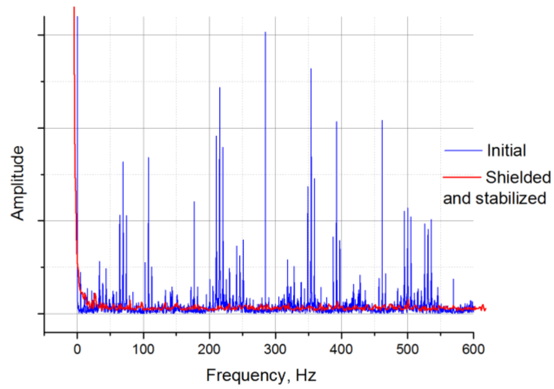

Figure 21 Noise frequency response before and after amplifier modification

3. Defect properties investigation

After defect localization visual evaluation of quench position should be done. For these purposes in the FLA/ILC HiGrade laboratory OBACHT and replica microscopy are used. They are described further.

3.1. OBAHT system

For visual control of cavity surface **O**ptical **B**ench for **A**utomated **C**avity Inspection with **H**igh Resolution on Short **T**ime Scales is used. OBACHT is a robot with camera and light source, installed on the rotating pole. System takes high resolution photographs of surface at discrete longitudinal and angular steps. These pictures combined represent a full image of cavity surface.

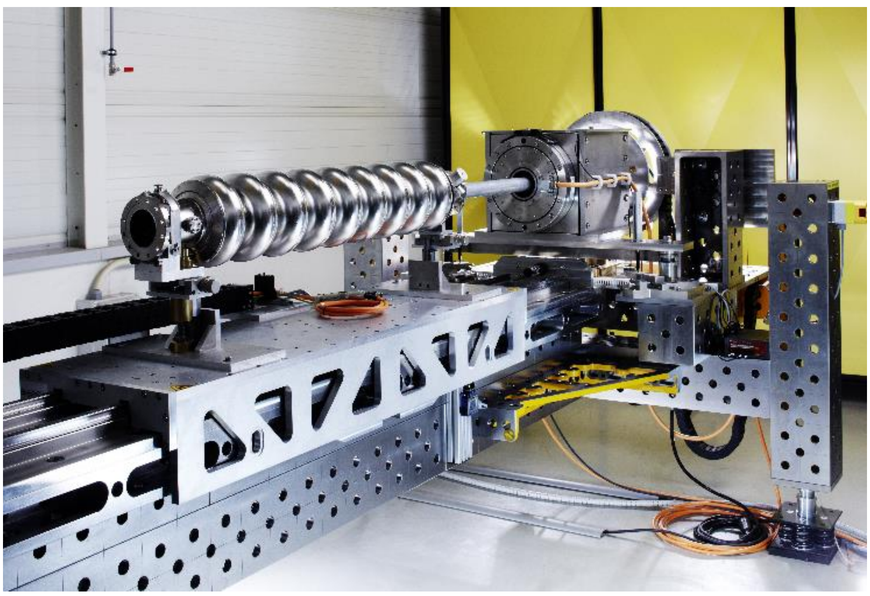
Figure 22 OBACHT setup

Information from T-mapping and Second Sound systems is used to determine possible cause of quench. Usually it is niobium surface defect or contamination by dust.

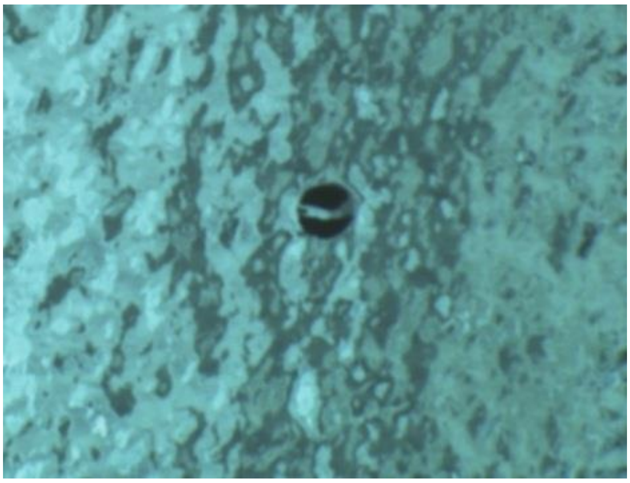

Figure 23 Photograph of surface defect taken by OBACHT

3.2. Replicas of defects

Images, provided by OBACHT are not informative in terms of vertical profile of defect. To obtain this information laser profilometry is needed. But it is not possible to use microscope in such a narrow space. To bypass this problem replica method was proposed.

Two-component silicon, poured on the defect area, solidifies and forms a footprint of cavity surface. This footprint, after extraction from the cavity, can be investigated by a microscope.

This process was proven reliable by testing comparing profiles of niobium peace (suitable for microscope investigation) and its replica under the scanning microscope. Microscope photographs of niobium and its replica surfaces are shown on figure 25.

Figure 25 Silicon replica of cavity welding seam

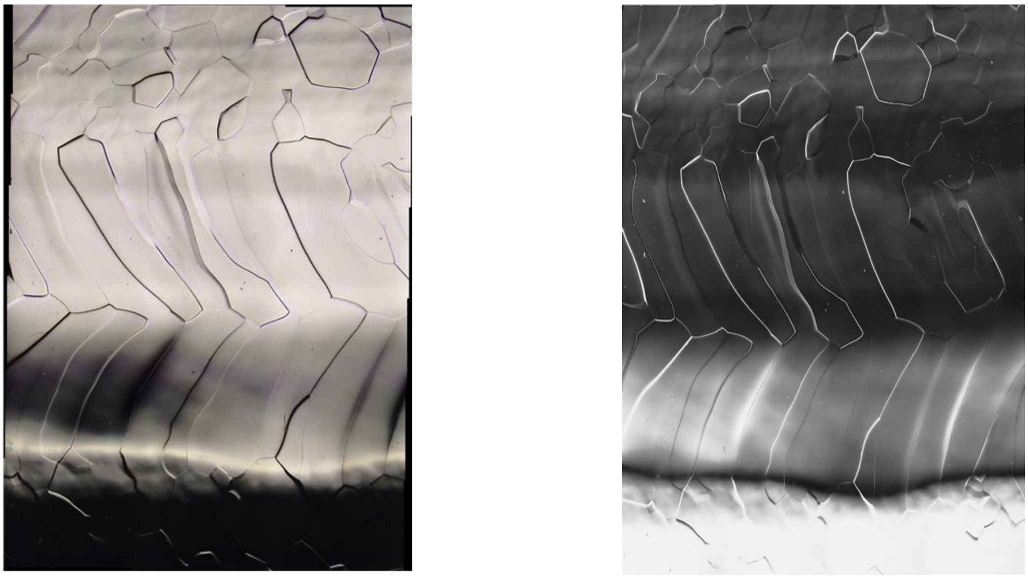

Figure 26 Microscope photography of niobium surface (left)
and of its replica (right)

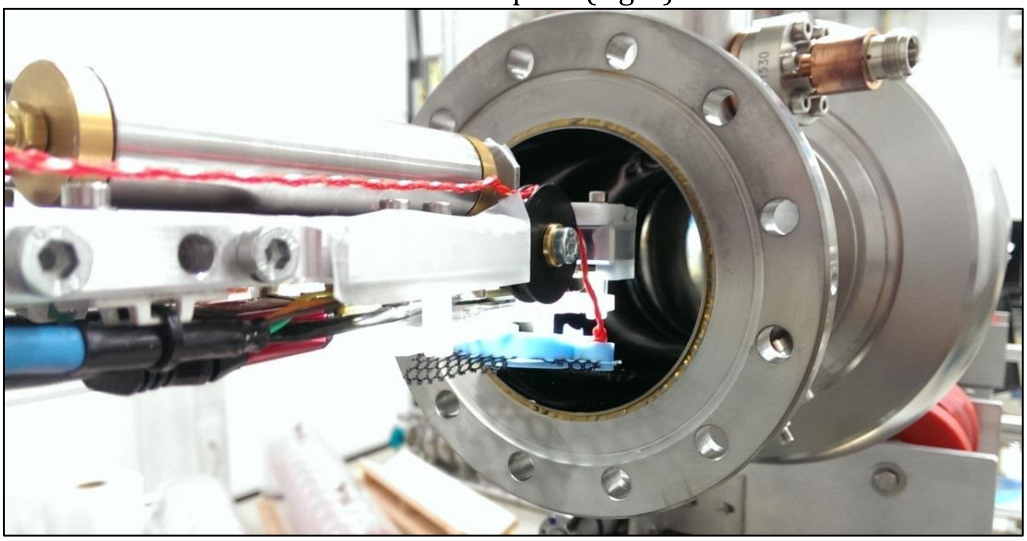

Figure 27 Replica tool

Advantage of replica microscopy is ability to assemble a three dimensional images of surface and vertical profiles of selected areas from laser profilometry (Figure 27).

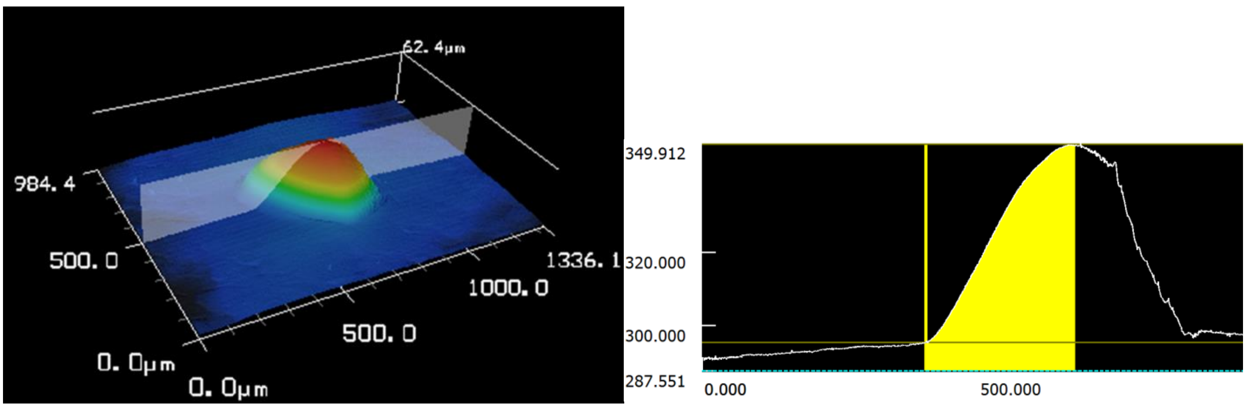

Figure 28 3D picture of surface defect (on the left) and its vertical profile (on the right)

4. Defects removal

After the defect localization, its removal method is chosen. In FLA/ILC HiGrade laboratory local grinding and centrifuge method of surface polishing are investigated.

4.1. Centrifuge polishing

Figure 29 Centrifuge barrel for nine-cell TESLA cavity polishing

Centrifuge polishing is done by friction of polishing media over the surface of cavity. To achieve required surface roughness four different polishing medias are used.

- First step
  First step uses mixture of one-centimiter stones with ultrapure water and anti-coagulation agent.

Figure 30 Photograph of stone, used for first polishing step

- Second step
  Second step uses mixture of 1 centimiter plastic pieces with ultrapure water and anti-coagulation agent.

Figure 31 Photograph of plastic piece, used for second polishing step

- Third step
  Third step uses mixture of alumina mesh with granule size of 15 μm with ultrapure water. half-centimiter blocks of wood are used for additional weight.

a) 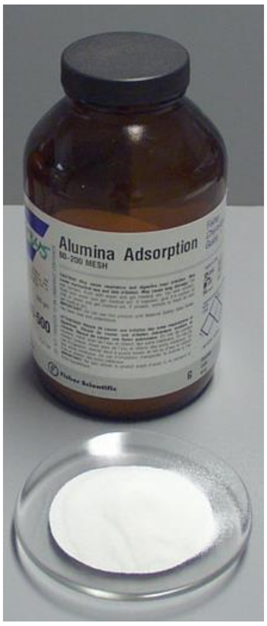

b) 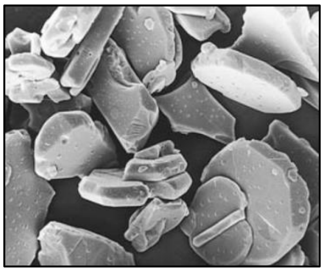
c) 

Figure 32 Photograph of alumina mesh (a), its magnified image (b) and wooden blocks (c), used for third polishing step

- Fourth step
  Fourth step uses mixture of colloidal silica with granule size of 40 nm with ultrapure water. Wooden blocks are used for additional weight.

a) 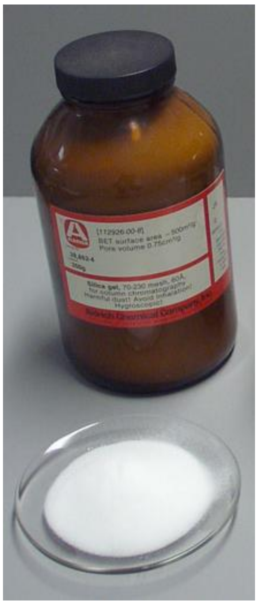
b) 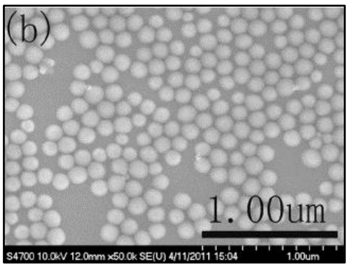

c) 

Figure 33 Photograph of silica (a), its magnified image (b) and wooden blocks (c), used for fourth polishing step

4.2. Diagnostics after polishing

To control polishing process FLA/ILC HiGrade laboratory uses several methods. They all allow to determine removed metal layer thickness with different accuracy and level of convenience.

- Weight measurement
  By subtracting mass of cavity before polishing from mass of cavity after polishing weight of removed metal is determined. Assuming uniform metal removal layer thickness of removed niobium can be calculated from 8 g per 1 µm ratio (for 9-cell 1.3 GHz niobium TESLA cavities)
- RF control
  Removal of metal from cavity surface leads to resonant frequency decrease. From this difference, thickness of removed layer can be calculated from 10 kHz per 1 µm ratio. Field profile and mode measurements allow to calculate removed layer for every cell and cell-part (equator, iris)
- Ultrasonic measurements
  From difference of propagation time of reflected sound waves from inner and outer surfaces of cavity, niobium wall thickness can be determined.

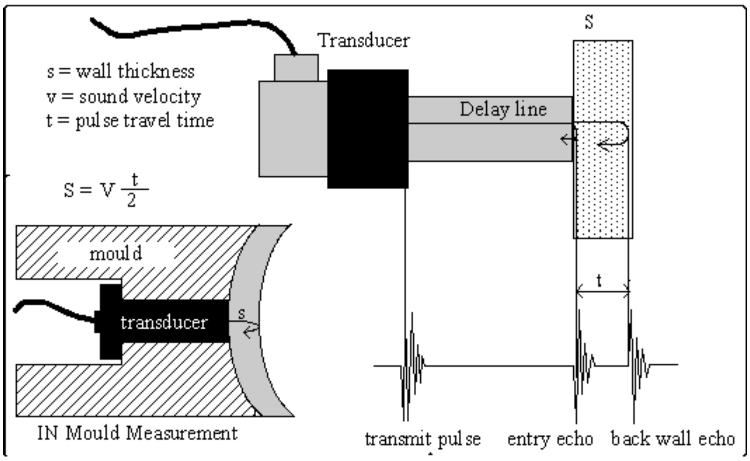

Figure 34 Ultrasound wall thickness measurement principal

- Replicas
  By controlling the welding seam profile with replica method, removed layer thickness can be determined. Also it gives the information about surface rougness and smoothness.

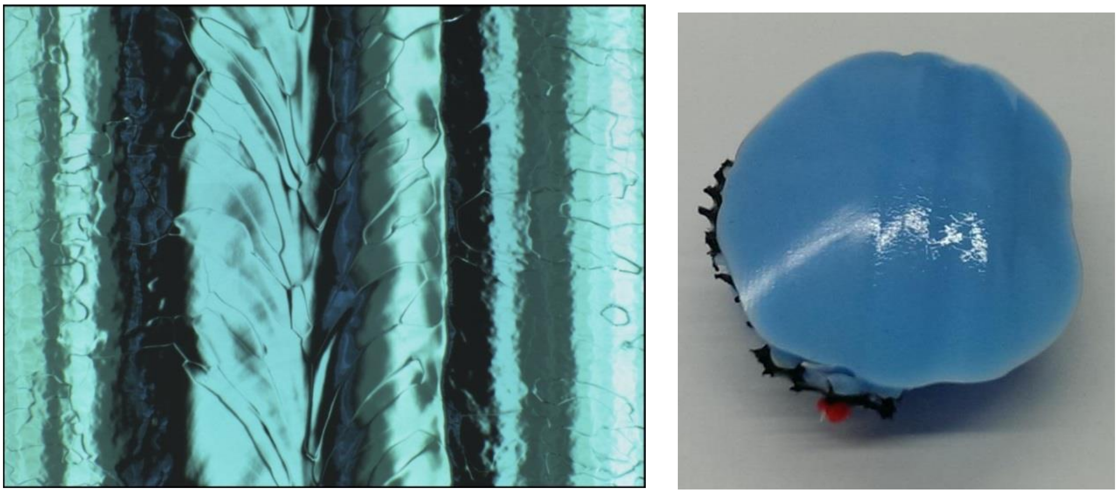

OBACHT image of welding seam (on the left) and its replica (on the right)

- Coupons

  By installing small pieces of niobium, called coupons, into the wall of cavity, removed layer thickness can be measured with microscope. The coupon can be investigated with SEM and EDX to determine surface microstructure and contamination by polishing media.

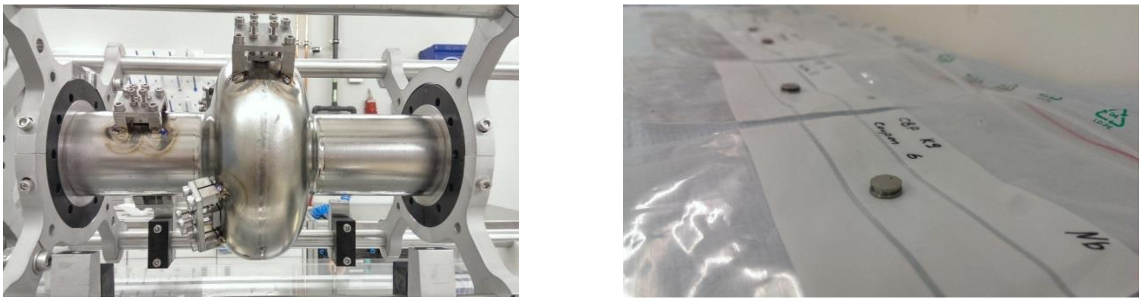

Figure 35 Single cell 1.3 GHz cavity with coupons

5. Summary

During the internship various tasks were done. T-mapping and Second Sound systems were assembled; modifications of Second sound system were made.

Q_0 over E_{acc} curves (cold test) were measured for several SRF cavities. Second sound and T-mapping measurements were made for cavities with quench.

Defects were found with OBACHT system, replicas of these defects were made and investigated using microscope. Polishing control of cavities via weight, RF and ultrasound measurements, replica and coupon methods.

6. References

[1] *European XFEL Design Report*
http://xfel.desy.de/technical_information/tdr/tdr/

[2] *ILC Design Report*
http://www.linearcollider.org/ILC/Publications/Technical-Design-Report

[3] *Superconducting accelerating cavities by Didenko A.N., Lalayan M.V., Sobenin N.P.*

[4] *The theory of superfluidity by Khalatnikov I. M.*

[5] *Hydrodynamics of a superfluid liquid by Patterman S.*

[6] *The two-fluid theory and second sound in liquid helium by Russell J. Donnelly, Physics Today*